Journal of Phytology 2024, 16: 163-168
doi: 10.25081/jp.2024.v16.8850
https://updatepublishing.com/journal/index.php/jp

Research Article

ISSN: 2075-6240

Sourcing antimicrobial agents from *Globimetula braunii*: An *in silico* molecular docking and dynamic approach

Ayodeji O. Oriola[1]*†, Pallab Kar[2]†, Adebola O. Oyedeji[1,2]

[1]Department of Chemical and Physical Sciences, Walter University, Mthatha, South Africa, [2]African Medicinal Flora and Fauna Research Niche, Walter Sisulu University, Mthatha, South Africa
†contributed equally to this work

ABSTRACT

The continued emergence of multi-drug resistance pathogens has been a major setback to lifting the burden of infectious diseases, especially bacterial illnesses. Natural- and/or nature-inspired compounds have so far become a therapeutic backbone on which many novel antibacterial agents are optimized. It is against this backdrop that we used an *in silico* molecular interaction-based approach to screen five previously identified compounds from *Globimetula braunii*, for lead inhibitors against bacterial illnesses. The compounds were chromatographed from the leaf ethyl acetate fraction and were characterized by spectroscopic means as 13,27-cycloursane (1), 13,27-cycloursan-3-one (2), methyl-3,5-dihydroxy-4-methoxybenzoate (3), 3-methyl-4-hydroxybenzoate (4), and 2-methoxyphenol (5). Upon their molecular docking at the active pocket of the *Staphylococcus aureus* gyrase B and the *Escherichia coli* DNA gyrase, 2 showed the highest binding affinities, with energy scores of -10 and -9.6 Kcal/mol. These were better than the standard antibiotics, Ampicillin (-7.5 and -8.0 Kcal/mol), and Ciprofloxacin (-6.9, -8.4 Kcal/mol). Further evaluation of the most promising compound 2 by molecular dynamics simulation showed the mean RMSD values of the 13,27-cycloursan-3-one - *E. coli* DNA gyrase protein complexes (complex 1) and 13,27-cycloursan-3-one - *S. aureus* gyrase B protein (complex 2) to be 0.7 and 0.9 Å respectively, attaining stability at 102 and 108 ns. In contrast, complexes 1 and 2's RMSF analysis revealed the fewest fluctuations and was generally stable over the course of the 120 ns. In conclusion, 13,27-cycloursan-3-one is unquestionably the most promising inhibitory candidate against the bacterial growth protein DNA gyrase, hence, it can be considered as a druggable substance against bacterial disease.

Received: March 04, 2024
Revised: July 01, 2024
Accepted: July 05, 2024
Published: September 09, 2024

***Corresponding Author:**
Ayodeji O. Oriola
E-mail: aoriola@wsu.ac.za

KEYWORDS: *Globimetula braunii*, Molecular docking, Molecular dynamics, Antimicrobials, 13,27-cyycloursan-3-one

INTRODUCTION

Bacterial strains that are resistant to the majority of antibiotics that have been found have emerged as a result of widespread antibiotic overuse. Due to the disruption of vast sensitive populations that compete with the resistant strains for food and space, the widespread and excessive use of antibiotics is largely to blame for the selective enrichment of the growth and spread of the resistant strains (Beveridge & Fyfe, 1995). Both genetic and non-genetic resistances are possible. Therefore, the proliferation of pathogenic microbes that have developed resistance to antibiotics to which they were previously susceptible is one of the possible challenges to medical sciences (Baker *et al.*, 2005). The term "multi-drug resistant" (MDR) refers to strains of bacteria that are resistant to many antibiotic classes. These strains are becoming more and more contagious worldwide (Paterson & van Duin, 2017). It has been noted that MDR strains that exhibit resistance to a prior antibiotic may not be able to be treated with currently available medications for the infection that this strain is causing (Flores-López *et al.*, 2016). Finding more recent classes of anti-infective substances that the organisms have not before come into touch with to make them responsive is one way to overcome resistance. It is imperative that such anti-infectives be used properly and under supervision to combat this resistant strain. This new substance may significantly contribute to slowing the rate of rapid dissemination (Beveridge & Fyfe, 1995). Consequently, a variety of workable, well-established methods are mostly employed to create anti-infective drugs, which would ideally get beyond the barrier of the cells' architectural elements. Therefore, there is a growing trend toward the use of naturally occurring phytocompounds for both the maintenance of human

health and the prevention and treatment of bacterial infections (Halliwell & Gutteridge, 1981).

Medicinal plants have become the backbone of herbal drugs in recent times. Natural substances and phytochemicals have been used as therapeutic agents to successfully cure serious illnesses. *Globimetula braunii* is a hemiparasitic plant belonging to the family Loranthaceae and distributed in various host plants from Ghana to Nigeria (Muhammad *et al.*, 2020). It has been found that *G. braunii* extract exhibits antibacterial action (Muhammad *et al.*, 2022). In our previous study, the isolation of compounds from *G. braunii* leaves, their antioxidant profiling as well as *in vitro* antimicrobial activity was reported (Oriola *et al.*, 2021). Therefore, in the current work using an *in silico* molecular interaction-based approach, we examined the reported phytocompounds isolated from *G. braunii* leaves (Figure 1), to evaluate their potential as inhibitors against bacterial illnesses.

MATERIALS AND METHODS

Plant Material and Extraction Method

Globimetula braunii was collected on the Obafemi Awolowo University (OAU) Campus, Ile-Ife, Nigeria. It was authenticated in the University Herbarium, (OAU), with a voucher number IFE 17729. The leaves were air-dried at room temperature (≈25 °C) and milled into powder and extracted with 80% EtOH by maceration method (Oriola *et al.*, 2021). Thereafter the ethanolic extract was subject to solvent-solvent extraction, by suspending the extract in distilled water and partitioning into *n*-hexane, ethyl acetate and *n*-butanol to afford the partition fractions.

Chromatographic Isolation and Spectroscopic Characterization of Compounds

The EtOAc fraction was chromatographed on a repeated column chromatography, using silica gel and Sephadex LH-20 as the stationary phase and organic solvent systems in increasing order of polarity (Oriola *et al.*, 2021), thus affording compounds 1-5. Spectroscopic analysis by nuclear magnetic resonance suggested the structures of the compounds.

In-silico Molecular Docking

Preparation and refinement of the protein and ligand structures

Robust molecular docking research was performed on the most notable and active chemicals extracted from *G. braunii* leaf extract using silica gel column chromatography, against growth proteins of pathogenic microorganisms. The protein of choice in this case is DNA gyrase, a crucial therapeutic target for illnesses involving bacterial infections. From the Protein Data Bank (http://www.rcsb.org), the PDB structure of *E. coli* DNA gyrase (PDB ID 6RKW; 6.60 Å resolution) (Broeck *et al.*, 2019) and *Staphylococcus aureus* gyrase B (PDB ID 4URM; 2.94 Å resolution) (Lu *et al.*, 2014) was obtained. Polar hydrogen atoms and Kollman charges were added to the protein structures after water atoms were removed in order to prepare them for docking in Auto Dock Tools.

The concerned phytocompounds namely 13,27-cycloursane, 13,27-cycloursan-3-one, methyl-3,5-dihydroxy-4-methoxybenzoate, 3-methyl-4-hydroxybenzoate and 2-methoxyphenol were downloaded from the NCBI PubChem

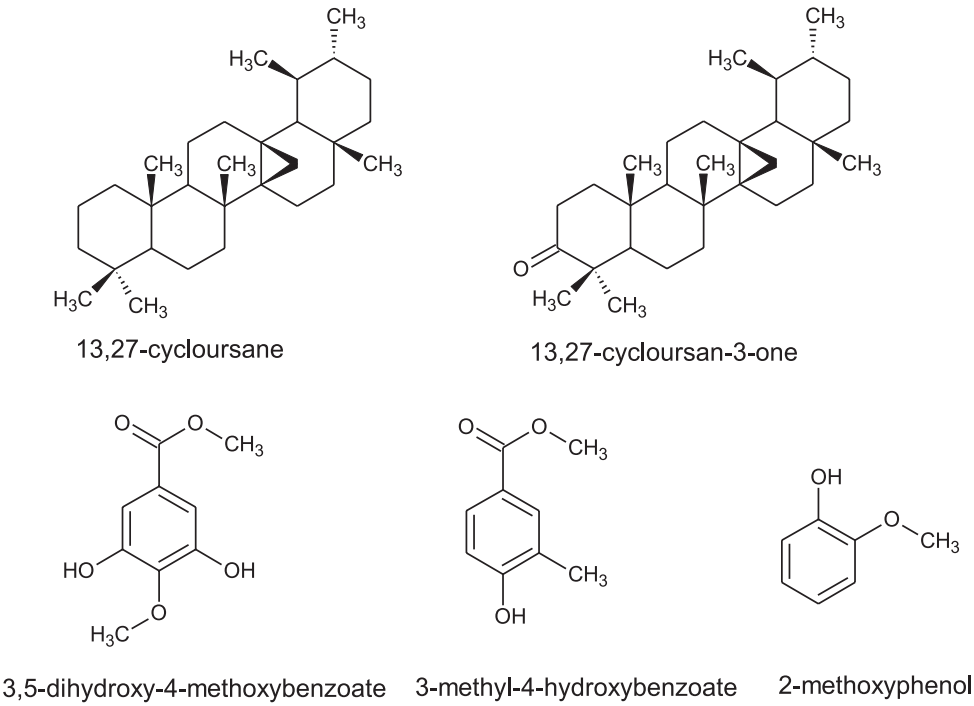

Figure 1: Isolated compounds from *Globimetula braunii* for *in silico* antibacterial studies

(https://pubchem.ncbi.nlm.nih.gov/). The ligand structures underwent energy minimization using the Gromos 96 force field after the PRODRG server (Schüttelkopf & van Aalten, 2004) was used to optimize their energy. Using Auto DockTools, Gasteiger charges were added to the ligand structures that had been produced (Jiang *et al.*, 2008).

Molecular docking

Molecular docking was performed using the AutoDock Vina software (Trott & Olson, 2010; Naidoo *et al.*, 2020). Using a grid-based docking technique, the ligands of interest were molecularly docked in the active binding sites of the relevant proteins using a stiff protein receptor and a flexible ligand docking methodology (Kar *et al.*, 2021, 2022a, b). To carry out the docking at the binding pockets of the relevant proteins, grid boxes with coordinates of 30, 30, and 30 in x, y, and z dimensions surrounding the active site residues were created (Naidoo *et al.*, 2020). Protein-Ligand Interaction Profiler (PLIP) web-server (Salentin *et al.*, 2015) and PyMol (version 1.7.4) software were used to perform interaction profiling and analysis on ligand-receptor complexes with the lowest binding scores and RMSD < 2.0 A (Naidoo *et al.*, 2020).

Molecular dynamics simulations

Molecular dynamics simulation (MDS) helps to precisely evaluate the possible stability of protein-ligand complexes and is a crucial step in confirming molecular docking results (Kar *et al.*, 2021). The compounds were subjected to MDS for 120 ns using the GROMACS (version 2019) force field parameters (GROMOS96 43a1) (Abraham *et al.*, 2015; Kar *et al.*, 2021, 2022a, b). Constant pressure and temperature (NPT) ensemble were used to set the equilibration stages (Elfiky & Azzam, 2020; Enayatkhani *et al.*, 2020; Umesh *et al.*, 2020). According to Umesh *et al.* (2020), the MD simulations were run a standard temperature of 300 K and pressure of 1.013 bars. An estimate of the conformational and structural stability of complexes was obtained through the analysis of root-mean-square-deviation/fluctuation (RMSD/F).

RESULTS AND DISCUSSION

Structure Elucidation

The molecular structures of the isolated compounds were elucidated based on previous report by Oriola *et al.* (2021) as shown:

13,27-cycloursane (1)

^{1}H-NMR (300 MHz, $CDCl_3$) δ ppm: 0.75 (3H, s, H-28), 0.89 (3H, d, J = 6.0 Hz, H-30), 0.98 (3H, s, H-26), 1.03 (3H, d, J = 3.0 Hz, H-29), 1.07 (3H, s, H-25), 1.20 (3H, s, H-24), 1.28 (3H, s, H-23); ^{13}C-NMR (75 MHz, $CDCl_3$) δ ppm: 39.27 (C-1), 22.30 (C-2), 29.71 (C-3), 30.02 (C-4), 59.51 (C-5), 18.26 (C-6), 41.32 (C-7), 39.72 (C-8), 58.25 (C-9), 37.47 (C-10), 30.52 (C-11), 41.55 (C-12), 38.32 (C-13), 42.16 (C-14), 36.03 (C-15), 32.46 (C-16), 53.12 (C-17), 28.19 (C-18), 42.82 (C-19), 35.04 (C-20), 35.65 (C-21), 32.80 (C-22), 32.11 (C-23), 31.80 (C-24), 20.27 (C-25), 17.96 (C-26), 35.36 (C-27), 14.68 (C-28), 18.68 (C-29), 6.84 (C-30).

13,27-cycloursan-3-one (2)

^{1}H-NMR (300 MHz, $CDCl_3$) δ ppm: 0.75 (3H, s, H-28), 0.89 (3H, d, J = 6.0 Hz, H-30), 0.98 (3H, s, H-26), 1.03 (3H, d, J = 3.0 Hz, H-29), 1.07 (3H, s, H-25), 1.20 (3H, s, H-24), 1.28 (3H, s, H-23); 13C-NMR (75 MHz, CDCl3) δ ppm: 39.27 (C-1), 22.30 (C-2), 213.18 (C-3), 30.02 (C-4), 59.51 (C-5), 18.26 (C-6), 41.32 (C-7), 39.72 (C-8), 58.25 (C-9), 37.47 (C-10), 30.52 (C-11), 41.55 (C-12), 38.32 (C-13), 42.16 (C-14), 36.03 (C-15), 32.46 (C-16), 53.12 (C-17), 28.19 (C-18), 42.82 (C-19), 35.04 (C-20), 35.65 (C-21), 32.80 (C-22), 32.11 (C-23), 31.80 (C-24), 20.27 (C-25), 17.96 (C-26), 35.36 (C-27), 14.68 (C-28), 18.68 (C-29), 6.84 (C-30).

3,5-dihydroxy-4-methoxybenzoate (3)

^{1}H NMR: (300 MHz, MeOD) δ ppm: 3.85 (3H, s, H-1a), 3.91 (3H, d, J = 3.0 Hz, H-4a), 4.89 (1H, s, H-3, H-5), 7.36 (1H, s, H-2, H-6); ^{13}C NMR: (75 MHz, MeOD) δ ppm: 55.26 (C-4-methoxy), 59.72 (C-1-methoxy), 106.80 (C-3, C-5), 125.72 (C-1), 142.41 (C-4), 152.90 (C-2, C-6), 168.05 (C-1-ester).

3-methyl-4-hydroxybenzoate (4)

^{1}H NMR: (300 MHz, MeOD) δ ppm: 2.05 (3H, s, Me), 3.90 (3H, s, -OCH_3), 4.88 (1H, s, -OH), 6.83 (1H, d, J = 9.0 Hz, H-5), 7.21 (1H, s, H-2), 7.46 (1H, d, J = 6.0 Hz, H-6); ^{13}C-NMR: (75 MHz, MeOD) δ ppm: 20.35 (C-3, Me), 55.38 (C-1, -OCH3), 110.74 (C-2), 114.30 (C-5), 116.27 (C-6), 122.43 (C-1), 144.62 (C-3), 150.09 (C-4), 168.74 (C-1-carbonyl ester).

2-methoxyphenol (5)

^{1}H NMR: (300 MHz, MeOD) δ ppm: 3.91 (3H, s, H-2a), 4.87 (1H, s, H-1a), 6.73 (1H, dd, J = 9.0 Hz, H-3), 6.98 (1H, t, J = 3.0 Hz, H-4, H-5), 7.10 (1H, t, J = 3.0 Hz, H-6); 13C-NMR: (75 MHz, MeOD) δ ppm: 55.34 (C-6a), 102.52 (C-4), 108.17 (C-5), 114.83 (C-3), 129.39 (C-6), 144.55 (C-2), 147.65 (C-1).

In-silico Molecular Docking

The phytochemicals from *G. braunii* were molecularly docked at the active pocket of the *S. aureus* gyrase B and the *E. coli* DNA gyrase. The protein under investigation is called DNA gyrase, and it has been linked to therapeutic targets for illnesses involving bacterial infections (Eakin *et al.*, 2012). The class of enzymes known as topoisomerases, which control DNA topological transitions, includes DNA gyrase. It is responsible for catalyzing double-stranded closed-circular DNA's ATP-dependent negative supercoiling. Maintaining DNA structure during replication requires DNA gyrase. Cell death results from DNA synthesis disruption caused by inhibition of DNA gyrase. Since DNA gyrase is a necessary component of all bacteria, antibacterials

find it to be a desirable target (Reece & Maxwell, 1991; Eakin *et al.*, 2012). The detailed binding energy scores of all the concerned phytocompounds have been provided in Table 1. With a binding affinity of -10.0 kcal/mol and -9.6 kcal/mol in autodock vina, 13,27-cycloursan-3-one exhibits the highest outcomes in this instance according to the *in-silico* insight (Figures 2a & b). However, other interesting compounds, such as 13,27-cycloursane are not far behind (Figures 3a & b). The current work examines the manner of binding of the drugs ampicillin and ciprofloxacin, which are currently utilized to prevent bacterial infection by targeting the DNA gyrases of *E. coli* and *S. aureus*. Ampicillin displayed a binding energy score of -7.5 kcal/mol and -8.0 kcal/mol with the DNA gyrases of *E. coli* and *S. aureus*. whereas, ciprofloxacin showed a binding energy score of -6.9 kcal/mol and -8.4 kcal/mol with the DNA gyrases of *E. Coli* and *S. aureus*. The binding energy scores (Table 1) made it clear that the chemicals 13,27-cycloursan-3-one and 13,27-cycloursane had substantially higher binding potential in comparison to the medications, ampicillin and ciprofloxacin. Thus, we can conclude that the compounds 13,27-cycloursan-3-one and 13,27-cycloursane examined in this work have enough potency to be taken into consideration as possible medications or druggable substances against bacterial disease.

MD Simulations

The compound 13,27-cycloursan-3-one had the best interaction with the *E. coli* DNA gyrase and *S. aureus* gyrase B protein in terms of binding energy scores (Table 1). It was also predicted that the compound would be non-toxic. As a

Table 1: Binding energy scores and interaction profile of the phytocompounds with bacterial gyrase proteins

Compound Name	Microbial Protein's PDB ID	Binding Affinity (Kcal/mol)	Interacting Residues
13,27-cycloursane (1)	6RKW	-8.1	*Arg32*, Lys42*, *Val44*, ***Arg91***
	4URM	-8.4	*Pro87*, Lys 93*, *Ala108*, **Arg200**, *Glu201, Phe204,*
13,27-cycloursan-3-one (2)	6RKW	-10.0	*Glu381, Ala384, Val385, Leu417, Ala421, Ala422, Ala432,* **Arg433**, *Tyr448*
	4URM	-9.6	*Asp57, Ile86, Pro87,* ***Gln91****, Ile102*
3,5-dihydroxy-4-methoxybenzoate (3)	6RKW	-5.8	*Ile506*, **Asp498, Asp500**
	4URM	-6.1	***Arg84***, **Arg144**, ***Tyr192***, Arg217*, **Arg223**
3-methyl-4-hydroxybenzoate (4)	6RKW	-5.9	*Tyr21*, ***Ala773***, *Leu776*, **Gly782**, **Glu786**
	4URM	-6.1	***Asn54***, *Ile86*, **Ser128**
2-methoxyphenol (5)	6RKW	-5.0	*Leu446*, **Thr497**, **Asp498**, *Ile506,*
	4URM	-5.2	**Asp81**, *Ile86*
Ampicillin	6RKW	-7.5	*Ile450*, Asp459, Ser463, Ser464, *Val467, Leu474, Phe513*
	4URM	-8.0	***Asn54, Ile86***, *Ile102, Ile175*, Arg200*
Ciprofloxacin	6RKW	-6.9	Arg433*, **Phe441**, *Tyr448*
	4URM	-8.4	*Asn54*, **Ser55, Asp81**, *Ile86, Thr173*

Hydrophobic interactions are marked in italics, hydrogen bonds are highlighted in bold. Salt bridges indicated in *

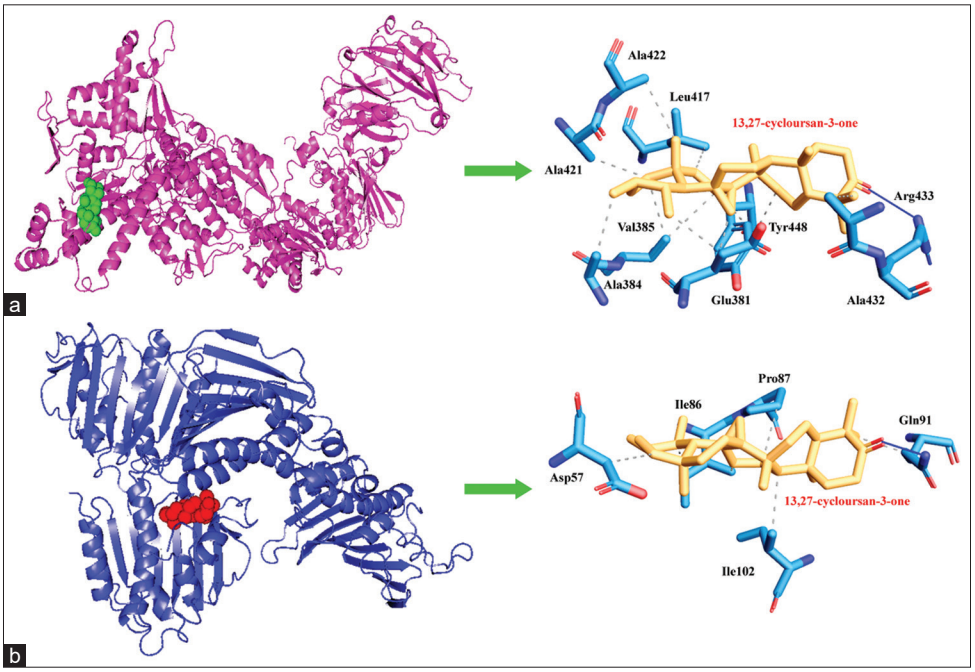

Figure 2: The mode of interaction of 13,27-cycloursan-3-one with a) *E. coli* DNA gyrase and b) *S. aureus* gyrase B protein. Pink ribbon represents the *E. coli* DNA gyrase protein and blue ribbon represents the *S. aureus* gyrase B protein. 13,27-cycloursan-3-one has been illustrated as a green and red sphere. Gray dashed and blue solid lines represent hydrophobic and hydrogen bonds respectively

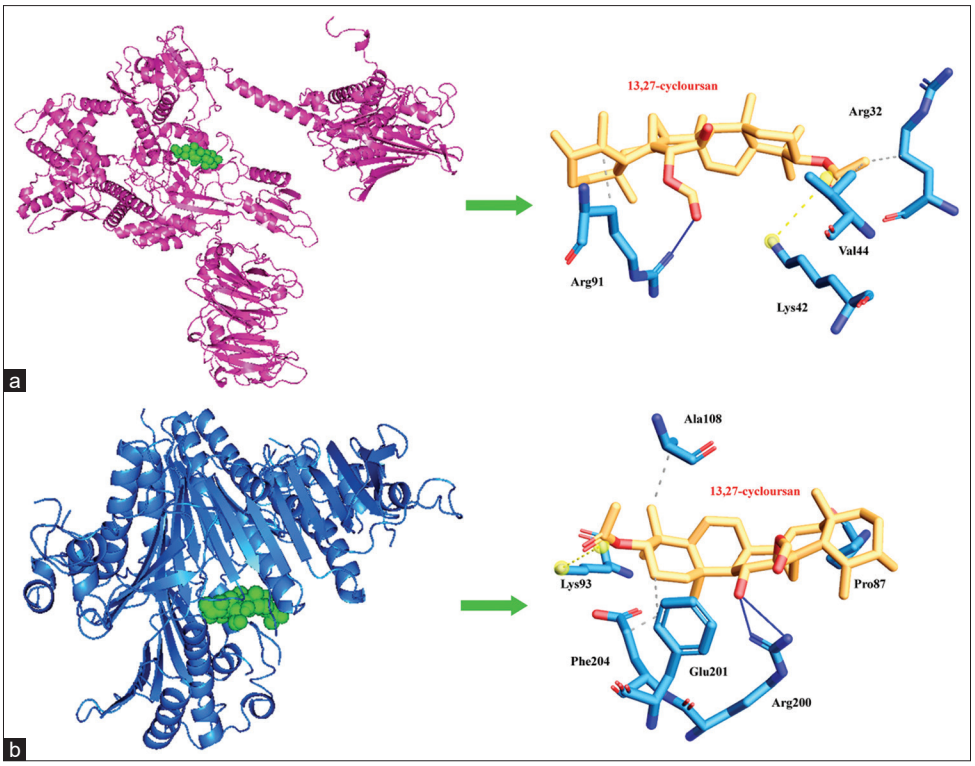

Figure 3: The mode of interaction of 13,27-cycloursane with a) *E. coli* DNA gyrase and b) *S. aureus* gyrase B protein. Pink ribbon represents the *E. coli* DNA gyrase protein and blue ribbon represents the *S. aureus* gyrase B protein. 13,27-cycloursan has been illustrated as a green sphere. Gray dashed, blue solid and yellow dashed lines represent hydrophobic, hydrogen bonds and salt bridges respectively

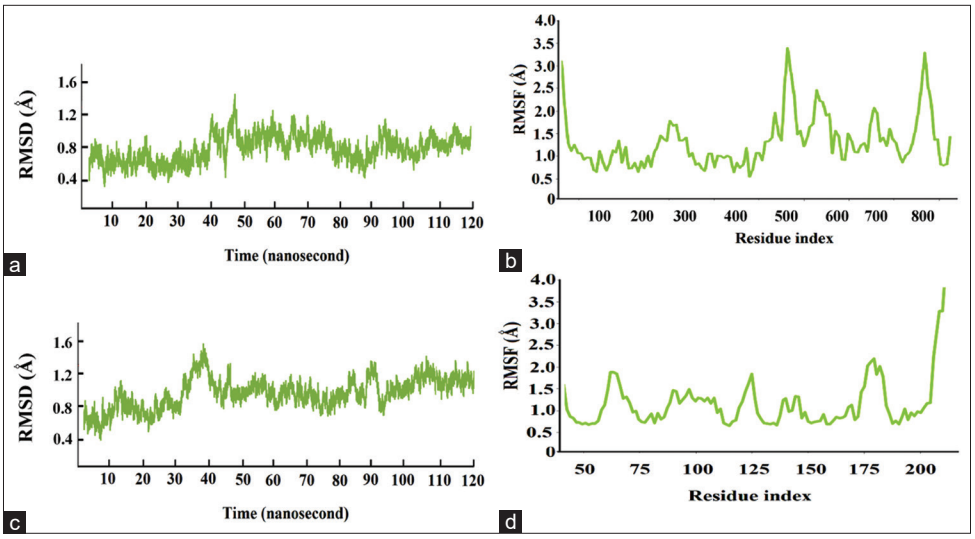

Figure 4: a) RMSD analysis of the complex 13,27-cycloursan-3-one - *E. coli* DNA gyrase protein. b) RMSF analysis of the complex 13,27-cycloursan-3-one - *E. coli* DNA gyrase protein. c) RMSD analysis of the complex 13,27-cycloursan-3-one - *S. aureus* gyrase B protein. d) RMSF analysis of the complex 13,27-cycloursan-3-one - *S. aureus* gyrase B protein

result, molecular dynamics (MD) simulations of the respective protein-ligand complexes were run for 120 ns. The mean RMSD values of the 13,27-cycloursan-3-one - *E. coli* DNA gyrase protein complexes (complex 1) and 13,27-cycloursan-3-one - *S. aureus* gyrase B protein (complex 2) was found to be 0.7 and 0.9 Å respectively, while the mean RMSF values were 0.75 and 0.9 Å for the corresponding complexes. The RMSD values of the C atoms in complexes 1 and 2 initially fluctuated, but after 102 and 108 ns they stabilized and remained in equilibrium (Figures 4a & c). In contrast, complexes 1 and 2's RMSF analysis revealed the fewest fluctuations and was generally stable over the course of the 120 ns MD simulations, reflecting the conformation stability of the corresponding complexes (Figures 4b & d).

CONCLUSION

Based on extensive molecular docking and MD simulations studies, the current research endeavor, which aimed to explore the inhibitory prospects of the phytocompounds isolated from *G. braunii*, revealed that 13,27-cycloursan-3-one was unquestionably the most promising inhibitory candidate against the bacterial growth protein DNA gyrase. So, we can conclude that the phytocompound 13,27-cycloursan-3-one has enough potency to be taken into consideration as a druggable substance against bacterial disease.

ACKNOWLEDGEMENT

The authors acknowledge the support of the National Research Foundation (NRF) South Africa through the NRF rated incentive grant. The Directorate of Research Development and Innovation, and the African Medicinal Flora and Fauna Research Niche, Walter Sisulu University, South Africa, are acknowledged for funding support.

REFERENCES

Abraham, M. J., Murtola, T., Schulz, R., Páll, S., Smith, J. C., Hess, B., & Lindahl, E. (2015). GROMACS: High performance molecular simulations through multi-level parallelism from laptops to supercomputers. *SoftwareX, 1*, 19-25. https://doi.org/10.1016/j.softx.2015.06.001

Baker, C., Pradhan, A., Pakstis, L., Pochan, D. J., & Shah, S. I. (2005). Synthesis and antibacterial properties of silver nanoparticles. *Journal of Nanoscience & Nanotechnology, 5*(2), 244-249. https://doi.org/10.1166/jnn.2005.034

Beveridge, T. J., & Fyfe, W. S. (1985). Metal □xation by bacterial cell walls. *Canadian Journal of Earth Sciences, 22*(12), 1893-1898. https://doi.org/10.1139/e85-204

Broeck, A. V., Lotz, C., Ortiz, J., & Lamour, V. (2019). Cryo-EM structure of the complete E. coli DNA gyrase nucleoprotein complex. *Nature Communications, 10*(1), 4935. https://doi.org/10.1038/s41467-019-12914-y

Eakin, A. E., Green, O., Hales, N., Walkup, G. K., Bist, S., Singh, A., Mullen, G., Bryant, J., Embrey, K., Gao, N., Breeze, A., Timms, D., Andrews, B., Uria-Nickelsen, M., Demeritt, J., Loch III, J. T., Hull, K., Blodgett, A., Illingworth, R. N., Sherer, B. (2012). Pyrrolamide DNA gyrase inhibitors: fragment-based nuclear magnetic resonance screening to identify antibacterial agents. *Antimicrobial Agents & Chemotherapy, 56*(3), 1240-1246. https://doi.org/10.1128/AAC.05485-11

Elfiky, A. A., & Azzam, E. B. (2020). Novel guanosine derivatives against MERS CoV polymerase: An *in silico* perspective. *Journal of Biomolecular Structure & Dynamics, 39*(8), 2923-2931. https://doi.org/10.1080/07391102.2020.1758789

Enayatkhani, M., Hasaniazad, M., Faezi, S., Guklani, H., Davoodian, P., Ahmadi, N., Einakian, M. A., Karmostaji, A., & Ahmadi, K. (2020). Reverse vaccinology approach to design a novel multi-epitope vaccine candidate against COVID-19: An *in silico* study. *Journal of Biomolecular Structure and Dynamics,* 39(8), 2857-2872. https://doi.org/10.1080/07391102.2020.1756411

Flores-López, N. S., Cortez-Valadez, M., Moreno-Ibarra, G. M., Larios-Rodríguez, E., Torres-Flores, E. I., Delgado-Beleño, Y., Martinez-Nuñez, C. E., Ramírez-Rodríguez, L. P., Arizpe-Chávez, H., Castro-Rosas, J., Ramirez-Bon, R., & Flores-Acosta, M. (2016). Silver nanoparticles and silver ions stabilized in NaCl nanocrystals. *Physica E: Low-dimensional Systems Nanostructures, 84*, 482-488. https://doi.org/10.1016/j.physe.2016.07.012

Halliwell, B., & Gutteridge, J. M. C. (1981). Formation of a thiobarbituric acid reactive substance from deoxyribose in the presence of iron salts. *FEBS Letter, 128*(2), 347-352. https://doi.org/10.1016/0014-5793(81)80114-7

Jiang, X., Kumar, K., Hu, X., Wallqvist, A., & Reifman, J. (2008). DOVIS 2.0: an efficient and easy to use parallel virtual screening tool based on AutoDock 4.0. *Chemistry Central Journal, 2*, 18. https://doi.org/10.1186/1752-153X-2-18

Kar, P., Kumar, V., Vellingiri, B., Sen, A., Jaishee, N., Anandraj, A., Malhotra, H., Bhattacharya, S., Mukhopadhyay, S., Kinoshita, M., Govindasamy, V., Roy, A., Naidoo, D., & Subramaniam, M. D. (2022a). Anisotine and amarogentin as promising inhibitory candidates against SARS-CoV-2 proteins: a computational investigation. *Journal of Biomolecular Structure and Dynamics, 40*(10), 4532-4542. https://doi.org/10.1080/07391102.2020.1860133

Kar, P., Saleh-E-n, M. M., Jaishee, N., Anandraj, A., Kormuth, E., Vellingiri, B., Angione, C., Rahman, P. K. S. M., Pillay, S., Sen A., Naidoo, D., Roy, A., & Choi, Y. E. (2022b). Computational profiling of natural compounds as promising inhibitors against the spike proteins of SARS-CoV-2 wild-type and the variants of concern, viral cell-entry process, and cytokine storm in COVID-19. *Journal of Cellular Biochemistry, 123*(5), 964-986. https://doi.org/10.1002/jcb.30243

Kar, P., Sharma, N. R., Singh, B., Sen, A., & Roy, A. (2021). Natural compounds from *Clerodendrum* spp. as possible therapeutic candidates against SARS-CoV-2: An *in silico* investigation. *Journal of Biomolecular Structure and Dynamics, 39*(13), 4774-4785. https://doi.org/10.1080/07391102.2020.1780947

Lu, J., Patel, S., Sharma, N., Soisson, S. M., Kishii, R., Takei, M., Fukuda, Y., Lumb, K. J., & Singh, S. B. (2014). Structures of kibdelomycin bound to *Staphylococcus aureus* GyrB and ParE showed a novel U-shaped binding mode. *ACS Chemical Biology, 9*(9), 2023-2031. https://doi.org/10.1021/cb5001197

Muhammad, K. J., Jamil, S., Basar, N., Arriffin, N. M., Idris, M. T., Jibril, S., & Akanji, F. T. (2022). Antioxidant, antimicrobial and antityrosinase activities of phytochemicals from the leaves of *Globimetula braunii* (Engler) Van Tiegh (Loranthaceae). *Bulletin of the Chemical Society of Ethiopia, 36*(2), 387-397. https://doi.org/10.4314/bcse.v36i2.12

Muhammad, K. J., Jamil, S., Basar, N., Sarker, S. D., & Mohammed, M. G. (2020). Globrauneine A–F: six new triterpenoid esters from the leaves of *Globimetula braunii. Natural Product Research, 34*(19), 2746-2753. https://doi.org/10.1080/14786419.2019.1586693

Naidoo, D., Roy, A., Kar, P., Mutanda, T., & Anandraj, A. (2020). Cyanobacterial metabolites as promising drug leads against the M^{pro} and PL^{pro} of SARS-CoV-2: An *in silico* analysis. *Journal of Biomolecular Structure & Dynamics, 39*(16), 6218-6230. https://doi.org/10.1080/07391102.2020.1794972

Oriola, A. O., Aladesanmi, A. J., Idowu, T. O., Akinwumi, F. O., Obuotor, E. M., Idowu, T., & Oyedeji, A. O. (2021). Ursane-type triterpenes, phenolics and phenolic derivatives from *Globimetula braunii* leaf. *Molecules, 26*(21), 6528. https://doi.org/10.3390/molecules26216528

Paterson, D. L., & van Duin, D., (2017). China's antibiotic resistance problems. *Lancet Infectious Diseases, 17*(4), 351-352. https://doi.org/10.1016/s1473-3099(17)30053-1

Reece, R. J., & Maxwell, A. (1991). DNA gyrase: structure and function. *Critical Reviews in Biochemistry and Molecular Biology, 26*(3-4), 335-375. https://doi.org/10.3109/10409239109114072

Salentin, S., Schreiber, S., Haupt, V. J., Adasme, M. F., & Schroeder, M. (2015). PLIP: fully automated protein-ligand interaction profiler. *Nucleic Acids Research, 43*(W1), W443-W447. https://doi.org/10.1093/nar/gkv315

Schüttelkopf, A. W., & van Aalten, D. M. F. (2004). PRODRG: a tool for high-throughput crystallography of protein–ligand complexes. *Acta Crystallographica Section D: Biological Crystallography, 60*(8), 1355-1363. https://doi.org/10.1107/s0907444904011679

Trott, O., & Olson, A. J. (2010). AutoDock Vina: Improving the speed and accuracy of docking with a new scoring function, efficient optimization, and multithreading. *Journal of Computational Chemistry, 31*(2), 455-461. https://doi.org/10.1002/jcc.21334

Umesh, Kundu, D., Selvaraj, C., Singh, S. K., & Dubey, V. K. (2020). Identification of new anti-nCoV drug chemical compounds from Indian spices exploiting SARS-CoV-2 main protease as target. *Journal of Biomolecular Structure and Dynamics, 39*(9), 3428-3434. https://doi.org/10.1080/07391102.2020.1763202